THE FAR FIELD OF A SUBMERGED LAMINAR JET: LINEAR HYDRODYNAMIC STABILITY

R.I. Mullyadzhanov, N.I. Yavorsky

Kutateladze Institute of Thermal Physics, Novosibirsk, Russian Federation

A linear stability problem for a submerged Landau – Squire jet has been considered. It was shown that in the space, the intrinsic perturbation amplitude varied as a power function of the spherical radius R, read from the motion source. It was established that the increment in the sinusoidal disturbance became more than that for axisymmetric one for Re $_D > 31$. The linear stability theory was applied to the value of the laminar-turbulent transition coordinate as a function of the Reynolds number. A model criterion for a laminar-turbulent transition in the far jet region was proposed. For the first time, this made it possible to obtain a good agreement between the theoretical results and experimental data for Re $_D < 2000$.

Key words: laminar jet, Landau solution, hydrodynamic stability, far field

Citation: R.I. Mullyadzhanov, N.I. Yavorsky, The far field of a submerged laminar jet: Linear hydrodynamic stability, St. Petersburg Polytechnical State University Journal. Physics and Mathematics. 11 (3) (2018) 84–94. DOI: 10.18721/JPM.11310

Introduction

Hydrodynamic stability theory studies the conditions under which one flow regime flow of a fluid or a gas is replaced by another [1 – 3]. Situations like that often happen in a wide range of natural phenomena and technical devices; therefore, new results in this field have numerous fundamental and practical applications. Free shear flows are one of the widest classes in hydrodynamics, with jet flows playing a central role. The classical problem on the stability of a circular flooded laminar jet issuing from a local source still has no definitive solution, stimulating further interest in this issue.

It was experimentally proved that a circular jet loses stability at relatively low flow velocities. Some of the first experiments on this problem, described in [4], were carried out by Schade. These experiments indicated that stable jet flow could be obtained at Reynolds numbers about several hundred. Further, Viilu [5] obtained in 1962 a result that somewhat contradicted Schade's data, determining the critical Reynolds number in the range of only 10.5 – 11.8. In the same year, A.J. Reynolds published the results of similar experiments [6], with a fairly detailed description of the scenarios dealing with the loss of flow stability.

The inlet conditions in such experiments are often modeled with a long tube; the velocity profile at the exit of this tube should be close to the parabolic Poiseuille profile. However, the outlet characteristics are highly dependent on the length of the tube nozzle.

More thorough studies of the outlet velocity profile were carried out in a relatively recent series of experiments [7, 8]. Measurements have shown that the length of the nozzle, which is about 200 channel diameters, is sufficient for forming a parabolic velocity profile up to Reynolds numbers of about 6700. It was also found that a non-axisymmetric mode, visualized in the cross-section, starts to develop at high flow velocities and close enough to the nozzle.

Lemanov et al. [9] studied submerged jets issuing from a nozzle with a length of 100D (D is the diameter of the tube). In addition, the flow was visualized and it was established that the region of steady laminar flow decreases with increasing Reynolds number. It was found (in agreement with the results of the previous authors) that sinusoidal perturbations start to evolve in the region located before the final turbulent transition of the jet. We are going to use the experimental data in this study for qualitative and quantitative comparison with the theory presented below.

Analytical study of this problem started with a paper by Batchelor and Gill [5], who found that only sinusoidal perturbation is an unstable mode in the far field in the inviscid case. How-

ever, the study also indicated that including the expansion of the jet downstream could slightly change the conclusions obtained using a plane-parallel approximation.

Tatsumi and Kakutani [10] note that stability analysis of non-parallel flows is not sufficiently developed in hydrodynamic stability theory that regards even such flows as jets and wakes as quasi-parallel. Ling and W.C. Reynolds [11] developed an approach taking into account flow expansion within the framework of perturbation theory. Garg [12] used a more general approach, applied only to Bickley's (two-dimensional) jet [13]. In contrast to the two-dimensional case, where the perturbation characteristics vary with the axial coordinate in a non-self-similar manner and some approximations have to be applied [14, 15], the general form of the perturbations in the three-dimensional case can be written based on self-similarity considerations. This analysis was first performed by Likhachev [16] for the Schlichting jet. Aside from unstable perturbations with $m = 1$ (m is the azimuthal wave number), unstable axisymmetric modes with $m = 0$ were detected. Even though axisymmetric perturbations turned out to be the most unstable only in a narrow range of rather small Reynolds numbers, this allowed a qualitatively explain the experimentally observed axisymmetric pulsations, described by W.C. Reynolds. Recall that the perturbations with $m = 1$ are the most dangerous for relatively large Re numbers. This analysis used the Schlichting solution, which is an equivalent of the exact Landau solution in the boundary layer approximation.

Shtern and Hussain [17] carried out a similar analysis for a Landau jet. Unlike previous studies, where the dependences of the perturbation v on the axial coordinate had the form $v \propto e^{ik(x)x}$ (x is the coordinate along the direction of the jet propagation, $k(x)$ is the axial wavenumber), where the maximum value of v decreases downstream, in this case, the perturbations were considered in the form $v \propto e^{ik(R)\ln R}$ (R is the spherical radius), based on a previous study for the two-dimensional setting [14, 15]. Thus, the authors discussed perturbations as a power function of R and obtained results similar to those presented in [16]. However, only neutral solutions were considered (the imaginary part of $k = 0$).

In addition to a non-standard dependence on the spatial coordinate, perturbations also do not have a purely exponential dependence on time. Thus, stability analysis is not modal, which follows from the fact that the characteristic time in the jet problem increases as $(R/|\mathbf{u}|) \propto R^2$ downstream, where $|\mathbf{u}|$ is the local velocity on the jet axis. The perturbations, whose wavelength and characteristic pulsation time also increase with increasing R, evolve together with the main flow [12]. Based on the conclusions of [16], we can assume that if we consider the spatial evolution of a small perturbation with a fixed frequency ω_0, the neutral curve $\omega_0(\mathrm{Re})$ and the scaling $\omega_0 \propto R^{-2}$ determine the variation range of R, where this perturbation grows, for a given value of Re.

This statement was confirmed by three-dimensional calculations of the stability problem [18]. Additionally, an important remark was made in [19]: calculations of the stability problem in unbounded domains are greatly complicated by numerical difficulties from the boundary conditions at the outlet; the latter can considerably distort the results.

It follows from this brief overview that using a self-similar form of disturbances allows to avoid the above-mentioned numerical difficulties. This statement is an additional argument in favor of the self-similar approach in this problem.

Problem statement

We study the evolution of perturbations $\mathbf{v}$ of a certain laminar velocity field $\mathbf{U}$; the total velocity field is represented as $\mathbf{u} = \mathbf{U} + \mathbf{v}$. Let us substitute this representation into Navier – Stokes equations and perform linearization assuming that the velocity perturbation amplitude is small compared with the main flow. We then obtain the following equation:

$$\frac{\partial \boldsymbol{v}}{\partial t} + (\boldsymbol{U} \cdot \nabla)\boldsymbol{v} + (\boldsymbol{v} \cdot \nabla)\boldsymbol{U} = -\frac{1}{\rho}\nabla\chi + \nu\Delta\boldsymbol{v}, \quad (1)$$

where χ is the pressure field perturbation, ν is the kinematic viscosity, ρ is the fluid density.

The velocity field of the main flow is described by the exact solution of Navier – Stokes equations that can be represented in spherical coordinates (R, θ, φ):

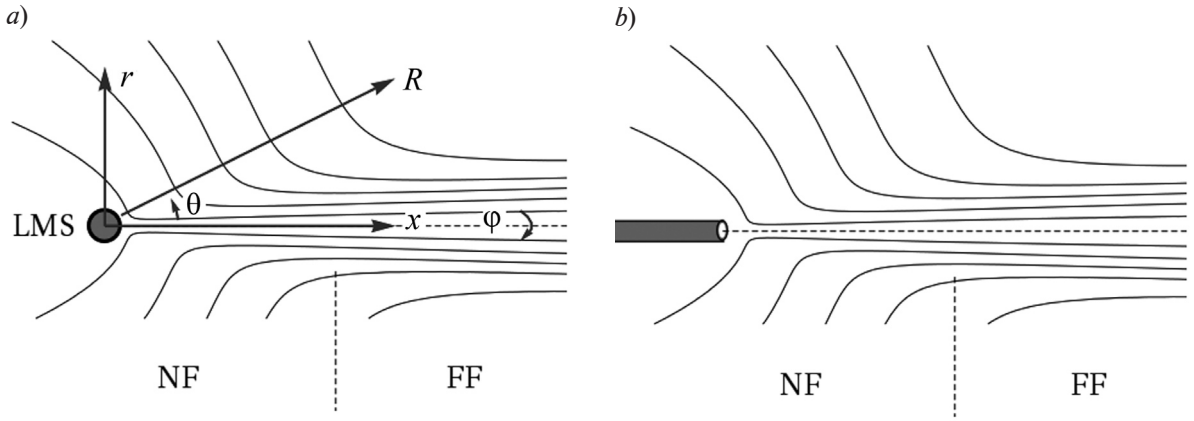

Fig. 1. Graphical representation of solution (3):
a is the idealized axisymmetric jet flow (streamlines are shown) caused by a local motion source (LMS), with coordinate systems (spherical and cylindrical); *b* is an implementation of such flow that is a fluid jet issuing from a long tube into a submerged region; NF, FF are the near and far fields, respectively

$$U_R = -\frac{\nu y'(\psi)}{R}, U_\theta = -\frac{\nu y(\psi)}{R\sqrt{1-\psi^2}},$$
$$U_\varphi = 0, y(\psi) = 2\frac{1-\psi^2}{A-\psi}, \quad (2)$$

where $\psi = \cos\theta$.

The parameter A is related as follows to the "momentum" P_x of the jet:

$$P_x = 16\pi\rho\nu^2 A\left[1 + \frac{4}{3(A^2-1)} - \frac{A}{2}\ln\frac{A+1}{A-1}\right], \quad (3)$$

This solution was obtained by Slyozkin [20], Landau [21] and Squire [22] and corresponds to jet flow caused by a point momentum source.

Fig. 1 shows a graphical representation of the solution obtained. This solution is used as the main flow in our study, since its direct comparison with experimental data yielded good agreement in the far field of the jet [23 – 25].

Since the problem statement does not include the characteristic dimension of length, for reasons of dimension, we are going to search for perturbations in the following class:

$$v_R = \frac{\nu}{R} f(\psi,\eta)e^{im\varphi},$$
$$v_\theta = -\frac{\nu}{R\sqrt{1-\psi^2}} g(\psi,\eta)e^{im\varphi}, \quad (4)$$
$$v_\varphi = \frac{\nu}{R} h(\psi,\eta)e^{im\varphi}, \chi = \frac{\rho\nu^2}{R^2} q(\psi,\eta)e^{im\varphi},$$

where the variable $\eta = \sqrt{(R/\nu t)}$.

Notably, the variables ψ and η were also used in analysis of two-dimensional [14, 15, 26, 27] and three-dimensional [28 – 30] conical flows. Using the method of variable separation, we can establish for $y = 0$ ($A \to \infty$) that the solution is expressed analytically in terms of Legendre polynomials with respect to the variable ψ and in terms of hypergeometric functions with respect to the variable η [31]. This actually means that the solution has a power dependence on η, which is not surprising as the representation of the velocity field of the main flow, constructed based on considerations of dimension, has a power dependence R^{-1}. Next, we transform the power dependence with a certain exponent n as follows:

$$\eta^n = (R/R_0)^n(\nu t/R_0^2)^{-n/2} = \exp[n\ln(R/R_0) - (n/2)\ln(\nu t/R_0^2)], \quad (5)$$

where R_0 – is some constant of the length dimension (radius of the inlet nozzle).

Evidently, if $y \neq 0$, it seems expedient to consider the problem on stability against perturbations in the form of waves in terms of new variables:

$$v = (\nu/R)v_0(\psi)\exp(ik\xi - i\omega\ln\tau + im\varphi),$$
$$\xi = \ln(R/R_0), \tau = \nu t/R_0^2, \quad (6)$$

where v_0 is a dimensionless vector depending only on the angle ψ; k and m are the radial and azimuthal dimensionless wavenumbers; ω

is the dimensionless frequency, τ is the dimensionless time.

Then the components of perturbations of the velocity and pressure fields have the form:

$$v_R = (\nu / R) f(\psi) \exp(ik\xi - i\omega \ln \tau + im\varphi),$$

$$v_\theta = \frac{\nu}{R\sqrt{1-\psi^2}} g(\psi) \exp(ik\xi - i\omega \ln \tau + im\varphi), \quad (7)$$

$$v_\varphi = \frac{\nu}{R\sqrt{1-\psi^2}} ih(\psi) \exp(ik\xi - i\omega \ln \tau + im\varphi),$$

$$\chi = \frac{\rho\nu^2}{R^2} q(\psi) \exp(ik\xi - i\omega \ln \tau + im\varphi),$$

where f, g, h, q are the dimensionless functions of only the angular variable ψ.

Substituting representation (7) into Eqs. (1), and making some transformations, we obtain a system of ordinary differential equations:

$$i\Omega f + \frac{2mh}{1-\psi^2} + (2-ik)q - 2g' + y''g + \frac{2yg}{1-\psi^2} - \left(2 + ik + k^2 + \frac{m^2}{1-\psi^2}\right) f - (2-ik)y'f - yf' - 2\psi f' + (1-\psi^2) f'' = 0;$$

$$i\Omega g + mh' + (1-\psi^2)(2f - (1+ik) f') - \left(ik + k^2 - \frac{m^2}{1-\psi^2}\right) g - (1-ik)y'g - \frac{2\psi yg}{1-\psi^2} - yg' - (1-\psi^2)q' = 0;$$

$$i\Omega h - mq + 2mf - \frac{2m\psi g}{1-\psi^2} - \left(ik + k + \frac{m^2}{1-\psi^2}\right) h + iky'h - yh' + (1-\psi^2)h'' = 0;$$

$$(1+ik) f + g' - \frac{mh}{1-\psi^2} = 0, \quad (8)$$

where $\Omega = \omega R^2 / (\nu t)$ is some constant parameter acting as the generalized frequency; it includes the dependence on the radius and time (proportional to the variable η^2).

The order of the derivative of the function g is reduced from the second to the first in the second equation of system (8) using the continuity equation. We should note that Eqs. (8) are identical to the equations obtained by Shtern and Hussain (who actually considered the exponential dependence of perturbation on time, or, more precisely, on $1/\eta^2$, used the far-field approximation ($\eta \to \infty$, which is equivalent to $\tau \to 0$) to derive the equations, and discarded some terms with high powers of τ). No approximations have been used in our study to derive these equations, except that Ω is assumed to be a constant parameter.

For complete statement of the problem, system of equations (8) should be supplemented with suitable boundary conditions. The following conditions imposed on the velocity field follow from representation (7):

$$g(\pm 1) = 0, h(\pm 1) = 0, \quad (9)$$

meeting the requirements that functions g and h be bounded.

Procedure of numerical solution

The procedure for numerical solution of the resulting system of equations is shown schematically in Fig. 2. Since the points $\psi = \pm 1.0$ are singular, we need to find the asymptotic expansion of the functions of the problem in their neighborhood of these points and shift the start of numerical integration. Asymptotic expansions of a certain test function Ψ in the neighborhood of singular points $\psi = \pm 1.0$ are used in the ranges $\psi \in [-1.0; \psi_c]$ and $[\psi_p; 1.0]$ (see expansion (10)). Next, two solutions of Eqs. (8) are constructed by numerical integration from ψ_c to ψ_m and from ψ_p to ψ_m. The values of the function Ψ and its derivatives should be kept continuous at the point ψ_m, in accordance with the order of the system of differential equations (see conditions (11)).

It can be shown for Legendre-type equations [32] that the functions of the problem are proportional to the factor $(1 - x^2)^{m/2}$ and a certain analytical (in the neighborhood of $\psi = \pm 1.0$) function, which, in turn, can be represented as a Taylor series.

Thus, some test function Ψ (f, g, h or q) in the neighborhood of the point $\psi = 1.0$ can be represented in the following form:

$$\Psi = (1-\psi^2)^{m/2} (\Psi_0 + \Psi_1(1-\psi) + \Psi_2(1-\psi^2) + \Psi_3(1-\psi^3) + ...), \quad (10)$$

where the complex-valued expansion coefficients $\Psi_0, \Psi_1, \Psi_2, \Psi_3$ are determined by substituting function (10) into system of equations

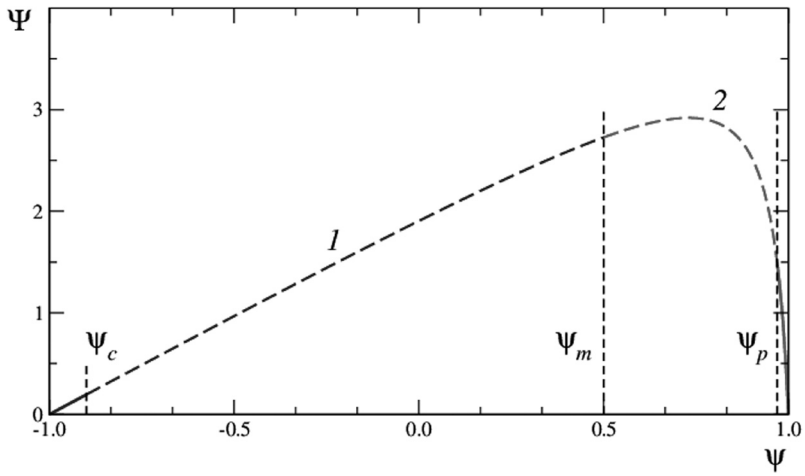

Fig. 2. Scheme of the numerical algorithm used:
Asymptotic expansions of a certain test function Ψ in the neighborhood of singular points $\psi = \pm 1.0$ are used in the ranges $\psi \in [-1{,}0;\ \psi_c]$ and $[\psi_p;\ 1{,}0]$ dashed curves *1*, *2* are the domains of further numerical integration; the condition that the values of the function ψ and its derivatives be continuous is imposed at ψ_m

(8). Some parameters remain undefined (free); these should be found by actually solving the spectral problem.

A decomposition similar to expression (10) can also be written in the neighborhood of the point $\psi = -1, 0$. Next, two numerical solutions need to be constructed for selected values of A (in the function y), Ω and a set of free parameters, and integration of Eqs. (8) starts from the points $\psi_c = -1.0 + \varepsilon_c$ and $\psi_p = 1.0 - \varepsilon_p$, where ε_c and ε_p are small parameters (in the range $10^{-5} - 10^{-3}$). The continuity conditions for the functions of the problem and their derivatives should be satisfied, in accordance with the order of the system of ordinary differential equations, at some point ψ_m ($\psi_m = 0.9$ for the solutions found below); the choice of this point does not affect the result. Namely, the following conditions should be fulfilled:

$$\begin{gathered} f_-(\psi_m) = f_+(\psi_m),\ f_-'(\psi_m) = f_+'(\psi_m), \\ g_-(\psi_m) = g_+(\psi_m), \\ h_-(\psi_m) = h_+(\psi_m),\ h_-'(\psi_m) = h_+'(\psi_m), \\ q_-(\psi_m) = q_+(\psi_m), \end{gathered} \qquad (11)$$

where plus and minus correspond to the solutions obtained by integrating the system of equations from the points ψ_p and ψ_c, respectively.

Conditions (11) are achieved by varying the free parameters and the wavenumber $k = k_{re} + ik_{im}$ using Newton's method. We used a similar calculation scheme in [33].

Results and discussion

Increasing perturbations (at $-k_{im} > 0$) were detected only for azimuthal wavenumbers $m = 0$ and $m = 1$, the same as in [17], which, however, discussed only neutral perturbations ($k_{im} = 0$). Thus, the k_{im}(Re) dependence was not analyzed in [17], which actually makes it possible for us to carry out a comprehensive comparison with experimental data, as will be shown below. It is convenient to use the Reynolds number, constructed from the velocity on the axis and the distance from the origin, in this problem:

$$\mathrm{Re} = \frac{U_R R}{\nu}\Big|_{\psi=1} = -y'(1) = -\frac{4}{A-1}, \qquad (12)$$

according to exact solution (2).

Fig. 3 shows the dispersion curves $-k_{im}(\Omega)$ for different Reynolds numbers Re and $m = 0$. As the Reynolds number increases above the critical value $\mathrm{Re}_{crit}^{m=0} = 26.20$, a range of Ω values appears, for which solutions exist, with $-k_{im} > 0$. Notably, $\mathrm{Re}_{crit}^{m=0} = 28.1$ was found in [17]. The small difference can be explained by the insufficiently accurate algorithm for calculating the spectral problem used in [17], where asymptotic expansions of the functions of the problem in the neighborhood of the points $\psi = \pm 1.0$ were not used.

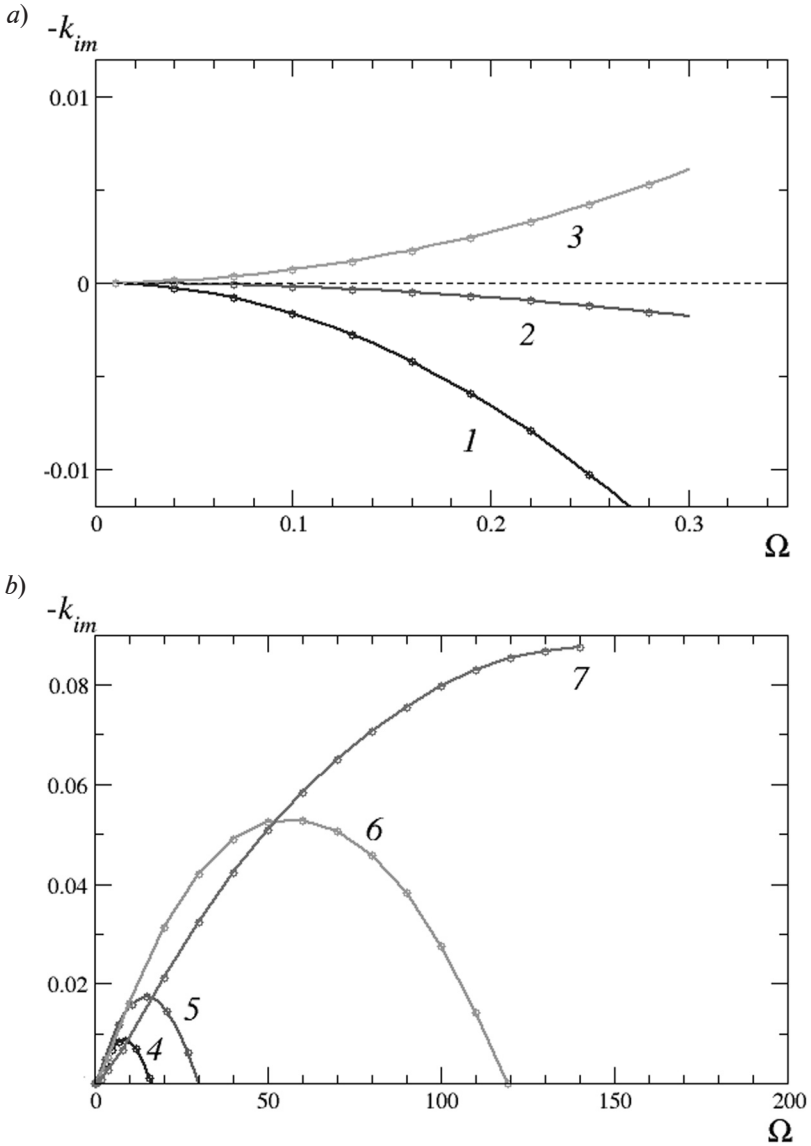

Fig. 3. Dispersion curves $-k_{im}(\Omega)$ in the ranges of the parameter Ω equal to (0 − 0.35) (*a*) and (0 − 200) (*b*), for the most unstable solution with $m = 0$, with different Reynolds numbers Re:
20 (*1*), 25 (*2*), 33,33 (*3*), 40 (*4*), 50 (*5*), 100 (*6*) и 200 (*7*)

The current statement of the problem allows studying the evolution of perturbations in the entire space, thanks to self-similarity of the main flow and the given perturbations, and is thus global. The ratio of the amplitude of perturbation velocity on the axis to the velocity of the main flow obeys the following relationship:

$$v_R / U_R = \left|[(\nu / R) f(1) e^{-k_{im}(\mathrm{Re})\xi}] \times \right.$$
$$\left. \times [(-\nu / R) y'(1)]^{-1} \right| \infty (R / R_0)^{-k_{im}(\mathrm{Re})}. \quad (13)$$

The perturbation amplitude algebraically grows or decays downstream relative to the main flow, depending on the distance measured from the origin. The growth rate is determined by the imaginary component of the wavenumber and depends on the Reynolds number. The absolute value of $-k_{im}(\mathrm{Re})$ turns out to be critical in this case.

Fig. 4 shows the dependence of the maximum value of $-k_{im}(\Omega)$, obtained for each dispersion curve, with different Re numbers. For

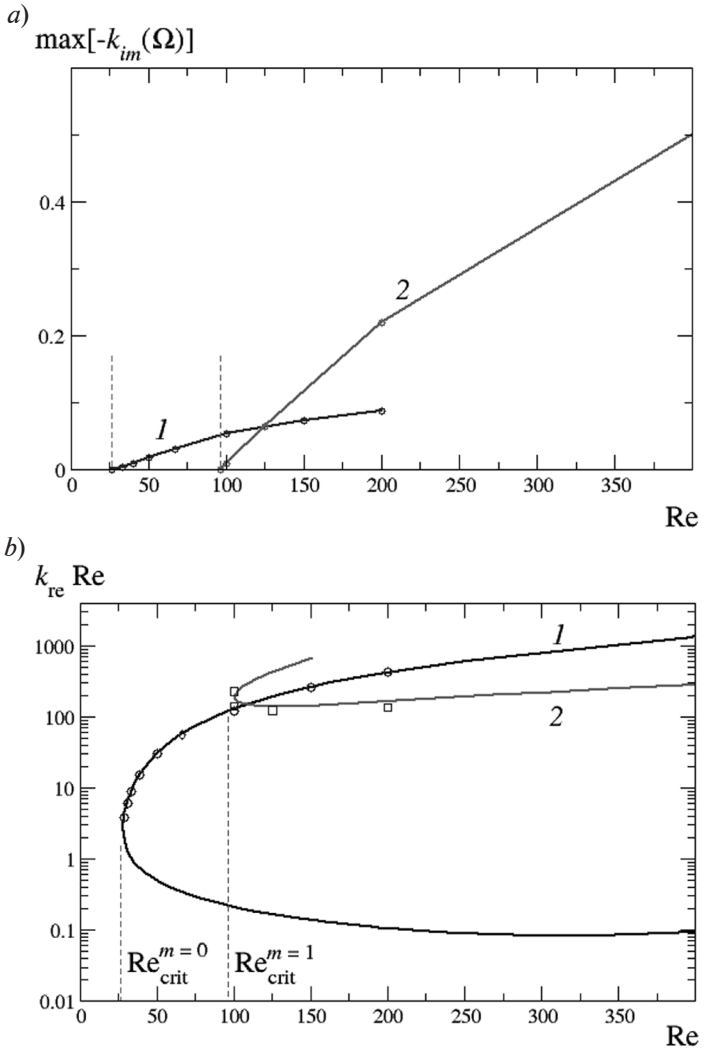

Fig. 4. Dependences of the maximum value of the imaginary component $-k_{im}$ (*a*) and the value of the real component k_{re}Re (*b*) of the wavenumber k on the Reynolds number for the most unstable solutions with $m = 0$ (*1*) and $m = 1$ (*2*). Fig. 4,*b* shows a comparison of the data in our study (symbols) with those in [17] (solid lines). The values $\mathrm{Re}_{crit}^{m=0} = 26.20$ and $\mathrm{Re}_{crit}^{m=1} = 96.29$ are marked with vertical dashes

instance, it is evident that even though positive $-k_{im}$ values exist for $\mathrm{Re} \le 40$, these values do not exceed 0.01. This suggests that the ratio of the perturbation amplitude to the main flow velocity on the axis increases by only 7 % (approximately) at a distance $R/R_0 = 10^3$, compared with this ratio at a distance $R/R_0 = 1$. With Re = 200, the peak $-k_{im}(\Omega)$ value on the dispersion curve is reached for $-k_{im} = 0.087$. The perturbation increases by 82 % at a distance $-k_{im}$ for these parameters.

Thus, we can conclude that, despite a mechanism of growing axisymmetric perturbations present in the given flow, the rate of such growth turns out to be extremely low. For this reason, axisymmetric perturbations can be characterized as neutrally stable in the first approximation. It is probably due to the weakly pronounced perturbation effect at $m = 0$ that only stable solutions are valid in the plane-parallel approximation. Fig. 4,*b* shows a comparison of the dependence of k_{re}Re on the Reynolds number Re, obtained in this study and in [17]. The curve representing the data from [17] demonstrably lacks a lower branch.

It can also be seen from Fig. 4,*b* that an

unstable solution for $m = 1$ appears if Re is increased to a value of the order of 100. The obtained value of the critical Reynolds number is $\mathrm{Re}_{crit}^{m=1} = 96.29$, which is slightly less than the corresponding value in [17] ($\mathrm{Re}_{crit}^{m=1} = 101$).

Comparing the maximum $-k_{im}(\Omega)$ values as functions of the Reynolds number Re with $m = 0$ and $m = 1$ indicates that the perturbation growth rate for $m = 1$ substantially exceeds that for $m = 0$ as the Reynolds number increases above a certain value. In this case, the maximum $-k_{im}$ values are approximately the same for $\mathrm{Re} \approx 120 - 130$.

The next stage of our study consisted in comparing the results of the above-described linear stability analysis with the experimental data given in the literature. We are going to find the relationship between the Reynolds number with the value of this number, used in experiments and numerical calculations, expressed by formula (12). The number constructed by the diameter of the exit nozzle $D = 2R_0$ and the mean flow rate U_b has the form

$$\mathrm{Re}_D = U_b D / \nu. \qquad (14)$$

Let us consider the parabolic velocity profile formed in the inlet nozzle. In cylindrical coordinates (x, r, φ) with the center in the middle of the exit section ($x = 0$), this profile has the following form:

$$U(R) = 2U_b(1 - R^2 / R_0^2), \qquad (15)$$

where R_0 is, the same as above, the radius of the tube.

The total momentum flux through the exit section is determined by the following relationship:

$$P_x = \oint \rho U^2(R) dS = 2\pi\rho \int_0^{R_0} U^2(R) R dR. \qquad (16)$$

Substituting formula (15) into relation (16), we obtain that

$$P_x = \frac{1}{3}\pi\rho\nu^2 \mathrm{Re}_D^2. \qquad (17)$$

Thus, we arrive at the following relationship:

$$\mathrm{Re}_D = \sqrt{\frac{3P_x}{\pi\rho\nu^2}}. \qquad (18)$$

Therefore, there is an explicit relationship between Re_D and Re (or between A and Re: $\mathrm{Re} = -4/(A - 1)$). The following asymptote can be written for large values of the Reynolds number:

$$\mathrm{Re}_D = \sqrt{8\mathrm{Re}} + \\ +\sqrt{2}(8 + \ln 8 - 3\ln \mathrm{Re})\mathrm{Re}^{-1/2} + \ldots, \mathrm{Re} \to \infty, \qquad (19)$$

with the first term often used in the literature ($\mathrm{Re}_D = \sqrt{8\mathrm{Re}}$).

The results of the analysis results for $m = 1$, obtained in this study, are compared in Table with the results of other authors. Notice that the

Table

Comparison of results obtained by different authors for analysis of linear stability of the Landau jet with the azimuthal wavenumber $m = 1$

Author	Re_{crit}	$\mathrm{Re}_{D,crit}$	$k_{re,crit}$	Ω_{crit}
V. Shtern, F. Hussain [17]	101.0	27.77	1.85	84.00
P.J. Morris [34]	177.1	37.64	2.12	86.66
O.A. Likhachev [16]	94.46	27.49	1.55	59.72
Our study	96.29	27.10	1.78	76.93

Notations: Re is the Reynolds number determined by formula (12), Re_D is the Reynolds number constructed from the diameter D of the exit nozzle; $k_{re,}$ is the real component of the wavenumber k; Ω is the parameter acting as the generalized frequency; the subscript "*crit*" indicates the critical value.

Notes. 1. The stability of the velocity profile was studied in [34] in a plane-parallel approximation using the Schlichting solution. 2. The same approach as in our study was used in [17].

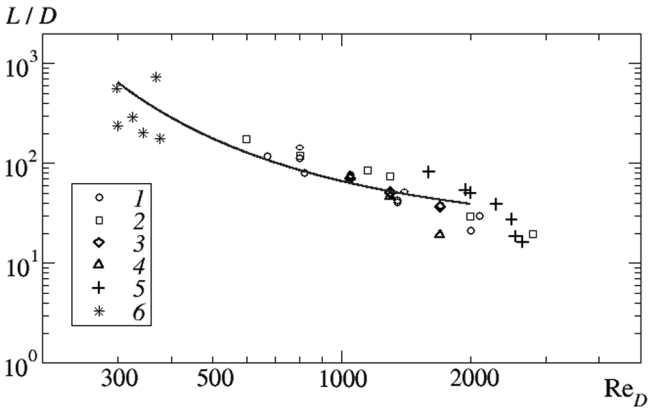

Fig. 5. Theoretical (line) and experimental (symbols) dependences of the distance at which the jet becomes turbulent versus the Reynolds number plotted for D.
The experimental data from [6, 9] were used, the theoretical curve was obtained in the present study. The diameter of the nozzle in [6] was $D = 0.32$ mm (symbols *6*). The experimental conditions in [9]: $D = 0.5$ mm (symbols *1*, *2*); 1.0 mm (*3*, *4*); 3.5 mm (*5*); velocity fluctuations were measured with a hot-wire anemometer (*2*, *4*) and visually (*1*, *3*, *5*)

critical Reynolds number Re_{crit} is significantly lower if the expansion of the jet is taken into account; however, the values of the Reynolds number $\mathrm{Re}_{D,crit}$ differ less in this case. The values of the real part of the wavenumber and the generalized frequency are also slightly lower. Nevertheless, the data obtained by Shtern and Hussain, as well as by Likhachev, are in good agreement with the results of our calculations.

Next, we estimated the distance L from the source of the jet, at which the perturbation amplitude takes some critical value, because the flow becomes turbulent. It is assumed in the calculations that perturbation grows by formula (13), in accordance with the given linear mechanism. Obviously, it is important to determine the criterion of laminar-turbulent transition in this case.

We assumed that the laminar-turbulent transition occurs when the perturbation amplitude significantly exceeds the local velocity at some point. By measuring this distance and using the dependences we found for $-k_{im}(\mathrm{Re})$ and formula (13), we obtained the dependence of L on Re.

Fig. 5 shows a comparison of the experimental data obtained by A.J. Reynolds [6] and by Lemanov et al. [9] with the theoretical dependence we have found (shown by a solid line).

The resulting expression has the form

$$L / D = 2,0 \cdot 10^{\alpha},$$
$$\alpha = 1 + 1 / (0,0081\mathrm{Re}_D{}^{0,8} - 0,11);$$

it was found by extrapolating the function $-k_{im}(\mathrm{Re})$ to higher values of the Reynolds number.

Comparison of theoretical and experimental results yields a good quantitative agreement, even though the turbulent processes, including the stage of nonlinear perturbation growth, are far more complex in reality, compared to the model. Importantly, turbulent fluctuations were observed in the flow from the tube even with $\mathrm{Re}_D > 2000$ (according to data obtained by Lemanov), which limits the range for comparison of theoretical and experimental data to $\mathrm{Re}_D < 2000$.

Conclusion

We have considered the linear stability problem for a submerged Landau – Squire jet. We have established that the amplitude of intrinsic perturbations spatially varies as a power function of the spherical radius R, read from the source of motion.

We have obtained a problem on the eigenvalues, which is solved numerically. Unstable perturbations were found for the first two azimuthal wavenumbers ($m = 0$ and 1); at the same time, the corresponding critical values of the Reynolds number, constructed

from the mean-flow velocity with a parabolic distribution inside the nozzle and its diameter, were

$\mathrm{Re}_D^{m=0} = 13.98$;

$\mathrm{Re}_D^{m=1} = 27.10$,

respectively.

We have confirmed that the increment for the growth of sinusoidal perturbations increases with values of $\mathrm{Re}_D > 31$, i.e., greater than that of axisymmetric perturbations.

We have proposed a model criterion for the laminar-turbulent transition in the far field of the jet, based on the fact that the ratio of the amplitude of the perturbation velocity to the main flow velocity spatially varies as a power function of R; the growth increment is known from the solution of the formulated spectral problem.

We have obtained for the first time a good agreement between the results of linear stability theory and the experimental data with $\mathrm{Re}_D < 2000$ for the coordinate of the laminar-turbulent transition as a function of the Reynolds number.

This study was financially supported by the grant of the Russian Science Foundation No. 14-19-01685.

REFERENCES

[1] **D.D. Joseph,** Stability of fluid motions, Vol. I. Springer-Verlag, Berlin-Heidelberg-New York, 1976.

[2] **P. Drazin, W. Reid,** Hydrodynamic stability. Cambridge University Press, Cambridge, 1981.

[3] **P.J. Schmid, D.S. Henningson,** Stability and transition in shear flows, Applied Mathematical Sciences, Springer, Berlin, 142 (2001).

[4] **G.K. Batchelor, A.E. Gill,** Analysis of the stability of axisymmetric jets, Journal of Fluid Mechanics. 14 (4) (1962) 529–551.

[5] **A. Viilu,** An experimental determination of the minimum Reynolds number for instability in a free jet, Journal of Applied Mechanics. 29 (3) (1962) 506–508.

[6] **A.J. Reynolds,** Observations of a liquid-into-liquid jet, Journal of Fluid Mechanics. 14 (4) (1962) 552–556.

[7] **G.V. Kozlov, G.R. Grek, A.M. Sorokin, Yu.A. Litvinenko,** Influence of initial conditions at the nozzle exit on the structure of round jet, Thermophysics and Aeromechanics. 15 (1) (2008) 55–68.

[8] **V.V. Kozlov, G.R. Grek, G.V. Kozlov, M.V. Litvinenko,** Subsonic round and plane jets in the transversal acoustic field, Vestnik NGU. Ser. Physics. 5(2) (2010) 28–42.

[9] **V.V. Lemanov, V.I. Terekhov, K.A. Sharov, A.A. Shumeyko,** An experimental study of submerged jets at low Reynolds numbers, Technical Physics Letters. 39 (5) (2013) 421–423.

[10] **T. Tatsumi, T. Kakutani,** The stability of a two-dimensional laminar jet, Journal of Fluid Mechanics. 4 (3) (1958) 261–275.

[11] **Chi-Hai Ling, W.C. Reynolds,** Non-parallel flow corrections for the stability of shear flows, Journal of Fluid Mechanics. 59 (3) (1973) 571–591.

[12] **V.K. Garg,** Spatial stability of the non-parallel Bickley jet, Journal of Fluid Mechanics. 102 (1981) 127–140.

[13] **W.G. Bickley,** The plane jet, The London, Edinburgh, and Dublin Philosophical Magazine and Journal of Science. 23 (156) (1937) 727–731.

[14] **K.K. Tam,** Linear stability of the non-parallel Bickley jet, Canadian Applied Mathematics Quarterly. 3 (1) (1995) 99–110.

[15] **A. McAlpine, P.G. Drazin,** On the spatio-temporal development of small perturbations of Jeffery–Hamel flows, Fluid Dynamics Research. 22 (4) (1998) 123–138.

[16] **O.A. Likhachev,** Analysis of stability in a self-similar circular jet with consideration of the nonparallel effect, Journal of Applied Mechanics and Technical Physics. 31 (4) (1990) 621–626.

[17] **V. Shtern, F. Hussain,** Effect of deceleration on jet instability, Journal of Fluid Mechanics. 480 (2003) 283–309.

[18] **X. Garnaud, L. Lesshafft, P.J. Schmid, P. Huerre,** Modal and transient dynamics of jet flows, Physics of Fluids. 25 (4) (2013) 044103.

[19] **L. Lesshafft,** Artificial eigenmodes in truncated flow domains, Theoretical and Computational Fluid Dynamics. 32 (3) (2018) 245–262.

[20] **N.A. Slyozkin,** Ob odnom sluchaye integriruyemosti polnykh differentsialnykh uravneniy dvizheniya vyazkoy zhidkosti [On a case of integrability of the complete differential equations of the motion of viscous fluid], Uchenyye zapiski MGU. (2) (1934) 89–90.

[21] **L.D. Landau,** Ob odnom novom tochnom reshenii uravneniy Navye –Stoksa [On an innovative exact solution to the Navier – Stokes equations], Doklady USSR AS. 43 (7) (1944) 299–301.

[22] **H.B. Squire,** The round laminar jet, The Quarterly Journal of Mechanics and Applied Mathematics. 4 (3) (1951) 321–329.

[23] **E.N. Andrade da C., L.C. Tsien,** The velocity-distribution in a liquid-into-liquid jet , Proceedings of the Physical Society. 49 (4) (1937) 381–391.

[24] **G.W. Rankin, K. Sridhar, M. Arulraja, K.R. Kumar,** An experimental investigation of laminar axisymmetric submerged jets, Journal of Fluid Mechanics. 133 (1983) 217–231.

[25] **B.J. Boersma, G. Brethouwer, F.T.M. Nieuwstadt,** A numerical investigation on the effect of the inflow conditions on the self-similar region of a round jet, Physics of Fluids. 10 (4) (1998) 899–909.

[26] **A.V. Shapeev,** Unsteady self-similar flow of a viscous incompressible fluid in a plane divergent channel, Fluid Dynamics. 39 (1) (2004) 36 –41.

[27] **A.V. Shapeev,** Issledovaniye smeshannoy spektralno-raznostnoy approksimatsii na primere zadachi o vyazkom techenii v diffuzore [Studies in the mixed spectral-difference approximation illustrated by the example of the problem on the viscous flow in a diffuser], Numerical Analysis and Applications. 8 (2) (2005) 149–162.

[28] **C. Sozou, W.M. Pickering,** The round laminar jet: the development of the flow field, Journal of Fluid Mechanics. 80 (4) (1977) 673–683.

[29] **C. Sozou,** Development of the flow field of a point force in an infinite fluid, Journal of Fluid Mechanics. 91 (3) (1979) 541–546.

[30] **B.J. Cantwell,** Transition in the axisymmetric jet, Journal of Fluid Mechanics. 104 (1981) 369–386.

[31] **R.I. Mullyadzhanov,** Zatoplennyye struynyye MGD techeniya [Submerged MHD jet flows], Thesis for Ph.D., Kutateladze Institute of Thermal Physics, SO RAS, Russian Federation, 2012.

[32] **V. Shtern, F. Hussain,** Instabilities of conical flows causing steady bifurcations, Journal of Fluid Mechanics. 366 (1998) 33–85.

[33] **R.I. Mullyadzhanov, N.I. Yavorsky,** On the self-similar exact MHD jet solution, Journal of Fluid Mechanics. 746 (2014) 5–30.

[34] **P.J. Morris,** The spatial viscous instability of axisymmetric jets, Journal of Fluid Mechanics. 77 (3) (1976) 511–529.

Received 23.03.2018, accepted 23.05.2018.

THE AUTHORS

MULLYADZHANOV Rustam I.
Kutateladze Institute of Thermal Physics
1 Acad. Lavrentiev Ave., Novosibirsk, 630090, Russian Federation
rustammul@gmail.com

YAVORSKY Nikolay I.
Kutateladze Institute of Thermal Physics
1 Acad. Lavrentiev Ave., Novosibirsk, 630090, Russian Federation
nick@itp.nsc.ru